

Fire behaviour of reinforced concrete slab strips strengthened with prestressed NSM-CFRP laminates

Adriana S. Azevedo^{a,*}, João P. Firmo^a, João R. Correia^a, Reza M. Firouz^b,
Joaquim A.O. Barros^b

^a CERIS, DECCivil, Instituto Superior Técnico, Universidade de Lisboa, Av. Rovisco Pais 1, 1049-001 Lisboa, Portugal

^b IRISE, University of Minho, Campus de Azurém, Av. da Universidade, 4800-058 Guimarães, Portugal

ARTICLE INFO

Keywords:

RC slabs
CFRP strengthening
NSM
Prestress
Fire behaviour

ABSTRACT

Carbon fibre reinforced polymer (CFRP) composites are now widely used to strengthen reinforced concrete (RC) structures. Among the strengthening systems available, near-surface mounted (NSM)-prestressed CFRP laminates offer several advantages, as they significantly increase the load carrying capacity and also the serviceability performance of RC structures. However, as for other CFRP systems, there is a concern about their behaviour at elevated temperature and under fire exposure due to the glass transition process undergone by their polymeric components. Nevertheless, the fire performance of NSM-prestressed-CFRP strengthening systems has not yet been investigated. This paper presents an experimental study about the fire resistance behaviour of RC slab strips strengthened with prestressed NSM-CFRP laminates; the slabs were simultaneously subjected to a mechanical (fire) load and the ISO 834 fire curve, and the influence of the following parameters on their fire resistance behaviour was assessed: (i) the prestress level (0 %, 25 % and 50 % of the CFRP tensile strength), and (ii) the presence of passive fire protection, comprising up to 48 mm thick calcium silicate (CS) boards. The results obtained showed that: (i) without fire protection, the strengthening system remained effective during a very low period of fire exposure, which significantly decreased with the prestress level, from 16 min (0 %) to less than 5 min (50 %); (ii) with fire protection, even with 50 % of prestress, the strengthening system remained effective for more than 120 min; and (iii) the “critical” temperatures in the anchorages of the strengthening systems were found to be about $2.5T_g$, $2.0T_g$ and $1.5T_g$ for the prestress levels of 0 %, 25 % and 50 %, respectively, with T_g being the glass transition temperature of the adhesive.

1. Introduction

Carbon fibre reinforced polymer (CFRP) systems are now widely used to strengthen reinforced concrete (RC) structures, due to the advantages they provide when compared to traditional systems, such as lightness, ease of installation, high strength-to-weight ratio and resistance to corrosion [1]. One of the techniques currently used to install CFRP systems in RC structures is the near-surface mounted (NSM) technique, which consists of bonding (typically using epoxy-based adhesives) CFRP laminates or rods inside slits pre-cut in the concrete cover [2]. This technique is very efficient in increasing the flexural and/or shear capacity of the strengthened RC members [3–8], due to the confinement provided by the surrounding concrete to the CFRP laminate, which prevents premature debonding mechanisms often found

with the externally bonded reinforcement (EBR) technique. However, the passive NSM technique (*i.e.* when the CFRP is not prestressed) does not significantly improve the serviceability and fatigue performance of RC members, namely the crack opening and deflections in service conditions.

Previous studies [9–16] have also shown that if NSM-CFRP laminates are prestressed, the serviceability performance of RC flexural members can be significantly improved compared with members comprising passive strengthening (no prestress). In fact, for prestress levels between 5 % and 60 %, the cracking and yielding loads have been reported to increase from 6 % to 310 %, and from 4 % to 69 %, respectively, for the lowest and highest prestress levels mentioned. These results, obtained at ambient temperature conditions, show the high efficiency of prestressed NSM-CFRP laminates/rods. However, the maximum load of the

* Corresponding author.

E-mail addresses: adriana.azevedo@tecnico.ulisboa.pt (A.S. Azevedo), joao.firmo@tecnico.ulisboa.pt (J.P. Firmo), joao.ramoa.correia@tecnico.ulisboa.pt (J.R. Correia), rezamf@civil.uminho.pt (R.M. Firouz), barros@civil.uminho.pt (J.A.O. Barros).

<https://doi.org/10.1016/j.engstruct.2023.116982>

strengthened member remains almost the same, irrespective of the prestress level, and the deflection at rupture decreases with the prestress level, penalizing its ductility.

Previous experimental and numerical studies [17–25] showed that passive CFRP strengthening systems are highly affected by high temperatures and fire exposure due to the polymeric nature of their constituent materials, namely the matrix of CFRP laminates or rods, and the epoxy adhesive. In fact, when their glass transition temperature (T_g) is attained or exceeded, these materials change from a vitreous state to a rubbery state, with a reduction of their stiffness and strength, as well as of the bond performance of the strengthening system. Fire resistance tests of RC members strengthened in flexure with passive-NSM-CFRP laminates/rods [21–24] showed that the strengthening system can lose its efficacy after periods of fire exposure as short as 15–16 min when no fire protection is applied; on the other hand, when using fire protection systems (comprising 30 mm thick rock-wool boards combined with 25 mm thick calcium silicate boards; 25 mm–50 mm thick calcium silicate boards, 10 mm–25 mm thick cementitious coating or 2 mm thick intumescent coating), the CFRP laminates or rods remained effective for much longer periods of fire exposure: (i) more than 30 min, when the CFRP anchorages were protected [22], (ii) more than 90 min, when a continuous fire protection was used at the exposed (strengthened) face of the strengthened specimens [21–24], and (iii) more than 110 min, when a thicker layer of fire protection was used at the anchorages zones combined with a thinner layer of fire protection in the centre of the span [22,24]. With this latter system, it has been shown that CFRP laminates behave like a cable system – the anchorages remain effective even when the CFRP laminate completely debonds from the concrete substrate along the centre zone of the span, allowing to increase significantly the period during which the strengthening system remains effective.

The above-mentioned studies confirm (i) the efficiency of prestressed NSM-CFRP strengthening systems at ambient temperature, (ii) the vulnerability to elevated temperature and fire of passive NSM-CFRP strengthening systems, and thus (iii) the need to apply passive fire protection systems to extend the period during which the structural efficacy of CFRP system is kept during fire exposure. Such vulnerability is expected to be more critical for prestressed systems, given the higher stress levels installed in both the CFRP components and CFRP-concrete interfaces. However, according to the knowledge of the authors, no studies have been conducted regarding the fire behaviour of RC members strengthened with prestressed CFRP laminates applied according to the NSM technique. Therefore, the present paper aims to bridge this research gap. To this end, an experimental study about the fire resistance behaviour of one-way RC slab strips strengthened in flexure with prestressed-NSM-CFRP laminates was conducted, in which the following two main aspects were investigated: (i) the influence of the prestress level installed in the CFRP laminates; and (ii) the effect of applying a fire protection system comprising calcium silicate (CS) boards.

2. Experimental programme

2.1. Test specimens

The experimental programme comprised flexural tests at ambient temperature and fire resistance tests on eight one-way RC slab strips (hereafter called “specimens”, for the sake of simplicity) strengthened with CFRP laminates applied according to the NSM technique (Fig. 1), with different prestress levels – more details about each test type are provided ahead. The flexural tests at ambient temperature were performed prior to the fire resistance tests in order to evaluate the efficacy of the CFRP strengthening system at ambient temperature conditions.

The following two main variables were studied: (i) the level of prestress applied in the CFRP laminates – 0 % (passive specimens), 25 % and 50 % of the CFRP tensile strength at ambient temperature; and (ii) the presence of fire protection (only in the fire resistance tests), composed by calcium silicate (CS) boards, with 48 mm of thickness at the anchorage zones and 24 mm of thickness at the centre of the span (Fig. 1b, Table 1). The fire protection thicknesses were defined based on results available in the literature concerning fire resistance tests (e.g. [22]) and numerical simulations [26] of NSM-CFRP strengthened RC members, where the effectiveness of these systems was demonstrated. In particular, it was shown that using a thicker layer of fire protection at the anchorage zones of the CFRP laminates prevents their premature debonding, while using a thinner layer at the central zone prevents the CFRP laminates from rupturing; this fire protection allows the CFRP (passive) strengthening system to remain effective, behaving like a cable.

In both types of tests, a non-strengthened RC slab strip was tested as reference (specimens RC). Table 1 identifies all specimens tested, indicating the type of test, the level of prestress, and the presence of fire protection; as an example, specimen F-50-P was tested in fire conditions (F), strengthened with NSM-CFRP laminates prestressed at 50 % of their tensile strength at ambient temperature (50), and insulated with the

Table 1
Details of tested specimens.

Specimen	Type of test	Prestress level (% ¹)	Fire protection (mm/mm)
A-RC	Flexural test at ambient temperature	–	–
A-0		0	–
A-25		25	–
A-50		50	–
F-RC	Fire resistance test	–	–
F-0		0	–
F-25		25	–
F-50		50	–
F-0-P		0	48 ² /24 ³
F-50-P		50	48 ² /24 ³

¹ Percentage of CFRP tensile strength at ambient temperature.

² Fire protection thickness at anchorage zones.

³ Fire protection thickness at centre of the span.

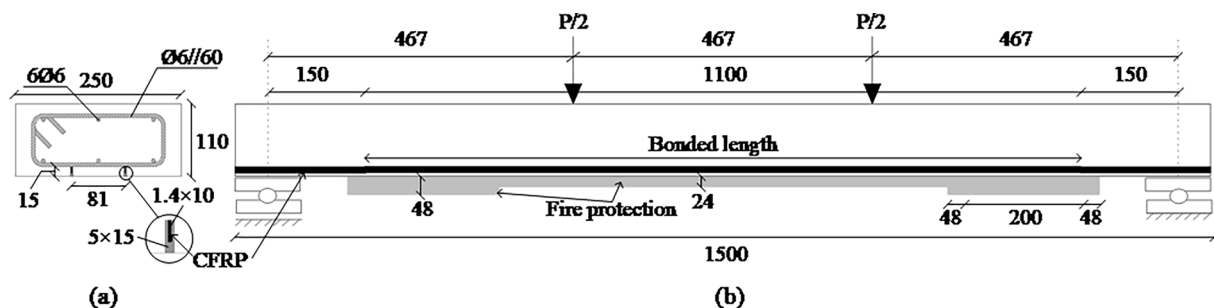


Fig. 1. (a) Midspan section geometry, (b) longitudinal scheme and fire protection geometry used (in grey). Dimensions in [mm].

above-mentioned fire protection system (P).

2.2. Materials

The specimens were cast with ready-mixed concrete produced with limestone aggregates and Portland cement type CEM II/A-L 42.5R (according to EN 197-1 [27]). The cure was performed in a humidified plastic enclosure for 5 days, after which the formwork was removed and the specimens were stored in the laboratory environment (indoor). The following mechanical properties of concrete were determined at the age when the flexural tests at ambient temperature were carried out (337 days): (i) average compressive strength in cubes of $f_{cm} = 29.5$ MPa (± 1.8 MPa, determined according to EN 12390-3 [28]), and (ii) average splitting tensile strength of $f_{ctm} = 1.7$ MPa (± 0.2 MPa, EN 12390-6 [29]).

The internal steel reinforcement consisted of six longitudinal rebars $\varnothing 6$ mm, three at the bottom layer and three at the top layer, and $\varnothing 6$ mm transverse stirrups spaced at 60 mm, adopted to prevent shear failure of the strengthened specimens (Fig. 1a). Their average mechanical properties (EN 10002-1 [30]) are as follows: (i) yield stress $f_{sym} = 594.4$ MPa (± 6.1 MPa), (ii) failure stress $f_{sum} = 686.7$ MPa (± 12.2 MPa), and (iii) elastic modulus $E_{sm} = 201.9$ GPa (± 16.9 GPa).

The strengthening system used in the experimental campaign comprised pultruded CFRP laminates and a two-component epoxy-based adhesive. The CFRP laminates had a cross section of $10 \text{ mm} \times 1.4 \text{ mm}$, and they were constituted by unidirectional carbon fibres (about 70 % in weight), embedded in an epoxy-vinylester resin matrix (commercial designation *S&P Laminates CFK 150/2000*). Two different CFRP laminate batches were used in the flexural tests at ambient temperature and in the fire resistance tests. Despite being supplied by the same manufacturer, some differences were found in their tensile properties. For the first batch, used for the flexural tests at ambient temperature, the average tensile properties (determined in [31], ISO 527-5 [32]) are as follows: (i) tensile strength $f_{fu} = 1909$ MPa (± 40 MPa), (ii) ultimate strain $\epsilon_{fu} = 11 \text{ ‰}$ ($\pm 0.48 \text{ ‰}$), and (iii) elastic modulus $E_f = 171$ GPa (± 3.7 GPa). For the second batch, used for the fire resistance tests, the average tensile properties (determined in [7], ISO 527-5 [32]) are as follows: (i) tensile strength $f_{fu} = 2850$ MPa (± 89 MPa), (ii) ultimate strain $\epsilon_{fu} = 16 \text{ ‰}$ ($\pm 0.28 \text{ ‰}$), and (iii) elastic modulus $E_f = 168$ GPa (± 4.5 GPa). The glass transition temperature of the CFRP laminates used in the fire resistance tests ($T_g = 83 \text{ °C}$, Fig. 2a) was determined in [7], through dynamic mechanical analysis (DMA, dual cantilever setup, heating rate of 1 °C/min , amplitude of 0.05 ‰ and frequency of 1 Hz), based on the onset of the storage modulus curve decay. Their decomposition temperature ($T_d = 380 \text{ °C}$, Fig. 2b) was also determined in [7] through thermogravimetric analysis (TGA, heating rate of 10 °C/min , in

air atmosphere), based on the midpoint temperature of the remaining mass curve.

The epoxy-based adhesive used to bond the CFRP laminates to the RC slab strips (commercial designation *S&P Resin 220*), comprised a relatively high content of additions and filler (about 70 % in mass) with relative coarse grading. Its average tensile properties at ambient temperature (determined in [20], ISO 527-2 [33]) are as follows: (i) elastic modulus $E_a = 10$ GPa, and (ii) tensile strength $\sigma_a = 14$ MPa. The T_g and T_d of the adhesive were determined according to the same methods used for the CFRP laminates, being $T_g = 46 \text{ °C}$ and $T_d = 380 \text{ °C}$ [7] (Fig. 2).

The fire protection system applied in specimens F-0-P and F-50-P comprised calcium silicate (CS) boards (commercial designation *Promatec-H500*), with the following properties at ambient temperature (provided by the manufacturer): (i) dry density of $\rho_{CS} = 870 \text{ kg/m}^3$, (ii) thermal conductivity of $\lambda_{CS} = 0.16 \text{ W/(m.K)}$, and (iii) specific heat capacity of $C_{p,CS} = 806 \text{ J/(kg.K)}$.

2.3. Preparation of specimens and prestress application

The preparation of the specimens for the application of the strengthening system comprised the following steps: (i) cutting the slits in the concrete cover ($15 \text{ mm} \times 5 \text{ mm}$, according to ACI 440.2R-17 [34] recommendations) using a diamond slit cutter; (ii) cleaning the slits with compressed air; (iii.1) for the passive strengthened specimens (0 % of prestress level), first the bonding adhesive was inserted in the slits and then the CFRP laminates were introduced; and (iii.2) for the prestressed strengthened specimens, first the CFRP laminates were inserted in the slits to apply the prestress force and then the bonding adhesive was introduced in the slits.

The prestress levels were defined based on previous studies [9–15] and ACI 440.4R-04 [35] recommendations; for all specimens, they were set as fractions (0 %, 25 % and 50 %) of the tensile strength of the CFRP laminates from the first batch ($f_{fu} = 1909$ MPa, used for the specimens tested at ambient temperature), corresponding to “initial” tensile strains in the CFRP of 0 %, 2.8 ‰ and 5.6 ‰. As mentioned in the previous section, the specimens used for the fire resistance tests were strengthened with CFRP laminates from a different batch that exhibited a higher tensile strength ($f_{fu} = 2850$ MPa). Consequently, the prestress levels of those specimens corresponded to 0 %, 17 % and 33 % of the average tensile strength of those laminates. Since the elastic modulus is almost the same in both batches, a similar stress state develops at the CFRP-adhesive-concrete interface, for both flexural tests at ambient temperature and fire resistance tests. For the sake of simplicity, hereafter the prestressed levels are referred to percentages of the tensile strength of the CFRP laminates from the first batch.

The prestress application process involved the following steps

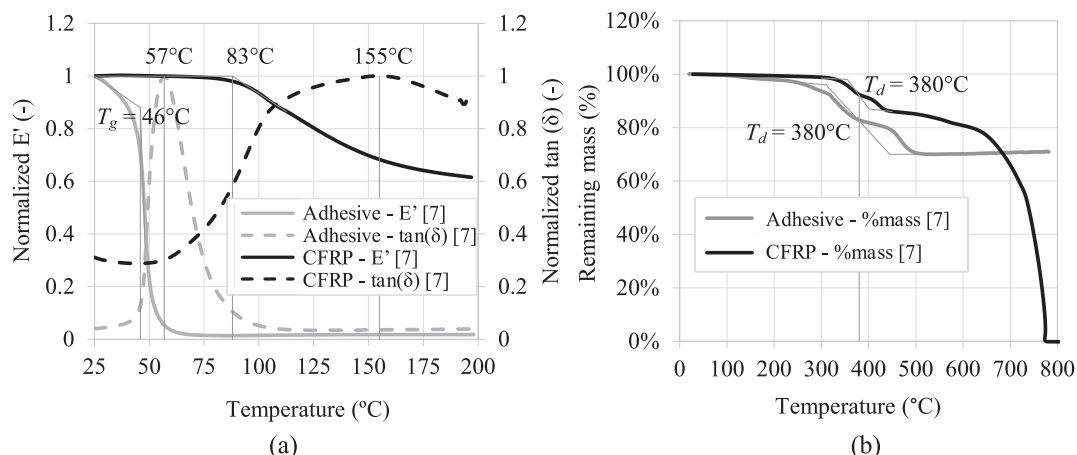


Fig. 2. Determination of the (a) glass transition temperature (T_g), and (b) decomposition temperature (T_d) of CFRP laminates and epoxy-based adhesive.

(similar to those adopted in [36]):

- (i) after aligning the slab strips inside a load reaction frame (built with steel profiles) and the CFRP laminates inside the slits of the concrete cover (Fig. 3), the predefined prestress forces were applied (≈ 0.02 kN/s). For this purpose, hydraulic jacks (load capacity between 120 kN and 200 kN) were placed outside the load reaction frame at one end of the CFRP laminates (active anchorage), while the other end of the CFRP laminates (passive anchorage) was fixed through steel plates also placed outside the load reaction frame (Fig. 3). During this stage, the applied prestress forces and the strains at the midspan and anchorage zones were monitored with a load cell of 100 kN capacity and electrical strain gauges, respectively;
- (ii) the bonding adhesive was applied inside the slits;
- (iii) after seven days of curing, the prestress forces were released, again monitoring the strains in the CFRP laminates at the midspan and at the anchorage zones. In this last stage, the maximum values of the prestress losses were below 2.1 %.

2.4. Flexural tests at ambient temperature

The specimens were monotonically loaded up to failure in a four-point bending configuration, as illustrated in Fig. 1b. The applied load and the midspan displacement were measured using a load cell and an electrical displacement transducer. Fig. 4a presents the load vs. midspan displacement curves of all specimens, in which three different stages can be identified: (i) elastic, (ii) elastic cracked, and (iii) elastoplastic.

As expected, in the first stage, the cracking load increased with the prestress level, respectively 20 % and 51 % for specimens A-25 and A-50 (25 % and 50 % of prestress), compared to the passively strengthened specimen (A-0). In the elastic cracked stage, the yielding loads also

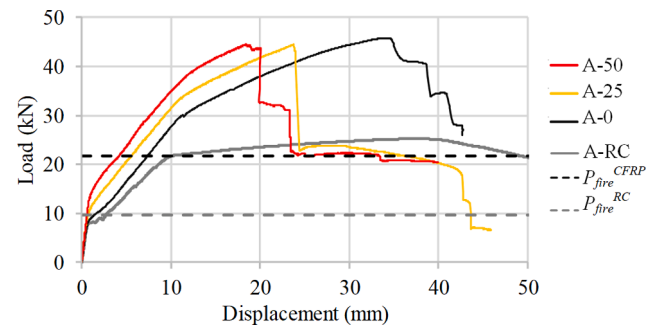


Fig. 4. (a) Load vs. midspan displacement curves (the fire load of the reference and strengthened specimens, P_{fire}^{RC} and P_{fire}^{CFRP} , are represented by the dashed lines, cf. Section 3.2).

increased with the prestress level, respectively 12 % and 28 % for specimens A-25 and A-50, compared to specimen A-0. After steel yielding, i.e. in the elastoplastic stage, the midspan displacement at failure decreased with the prestress level increase, respectively 32 % and 45 % for specimens A-25 and A-50, compared to specimen A-0, thus highlighting the typical ductility reduction of these strengthening systems when the prestress level is increased. Table 2 provides a summary of the results of these tests in terms of cracking load, yielding load, failure load and maximum displacement at failure.

Fig. 5a, b, c, and d shows the failure modes of specimens tested at ambient temperature. As expected, specimen RC (reference specimen, Fig. 5a) failed due to concrete crushing after steel yielding, while specimen A-0 (passive strengthening) presented flexural-shear failure triggered at the end of the CFRP laminates (Fig. 5b); this undesirable failure mode was caused by the high flexural strength increase provided

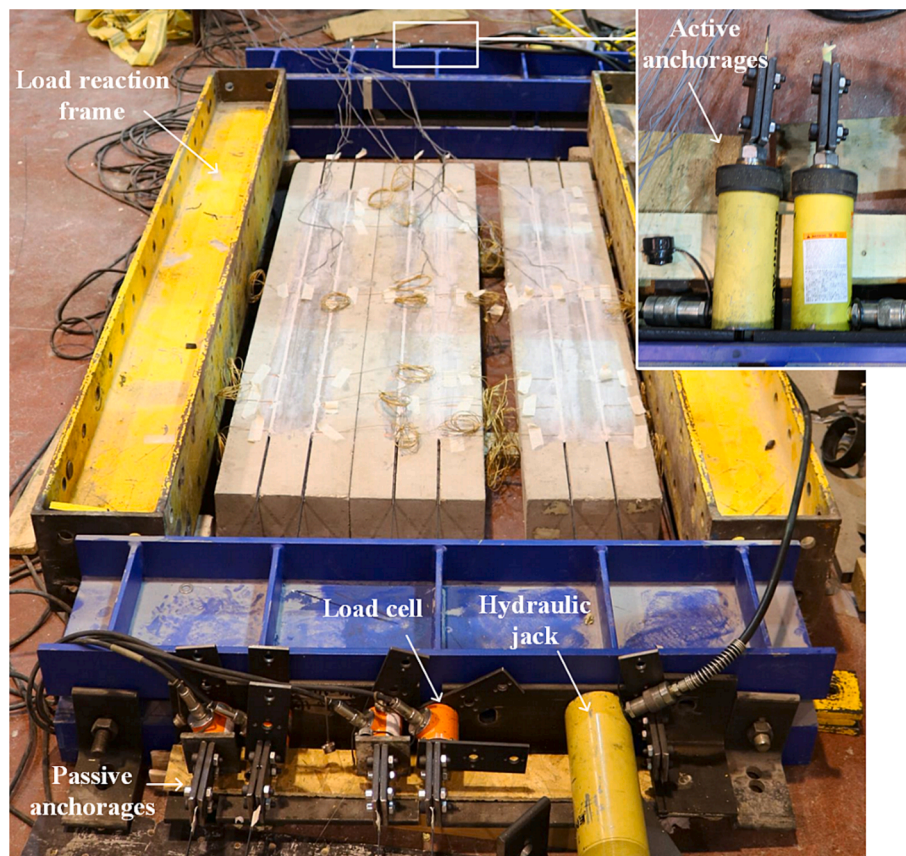


Fig. 3. Prestress application system.

Table 2

Tests results at ambient temperature: cracking, yielding, and failure loads and maximum midspan displacement.

Specimen	Cracking load (kN)	Yielding load (kN)	Failure load (kN)	Midspan displacement at maximum load (mm)
A-RC	8.0	21.5	25.3	38.0
A-0	8.9	30.1	45.8	34.1
A-25	10.7	33.8	43.9	23.7
A-50	13.4	38.6	44.2	18.9

by the strengthening system combined with the relatively low concrete strength (and, consequently, its low shear strength). Regarding the prestressed strengthened specimens (A-25 and A-50), both presented typical flexural failure modes, namely tensile rupture of the CFRP laminates in specimen A-25 (Fig. 5c), and pull-off of the CFRP laminates at the anchorages in specimen A-50 (Fig. 5d) – in these cases, shear failure did not precede the CFRP rupture/detachment due to the lower level of deformations in the slab strips, the less extensive concrete cracking, and the associated beneficial effects provided by the prestressed CFRP to the shear-carrying mechanisms (*i.e.* increased contribution of both aggregate interlock and uncracked concrete).

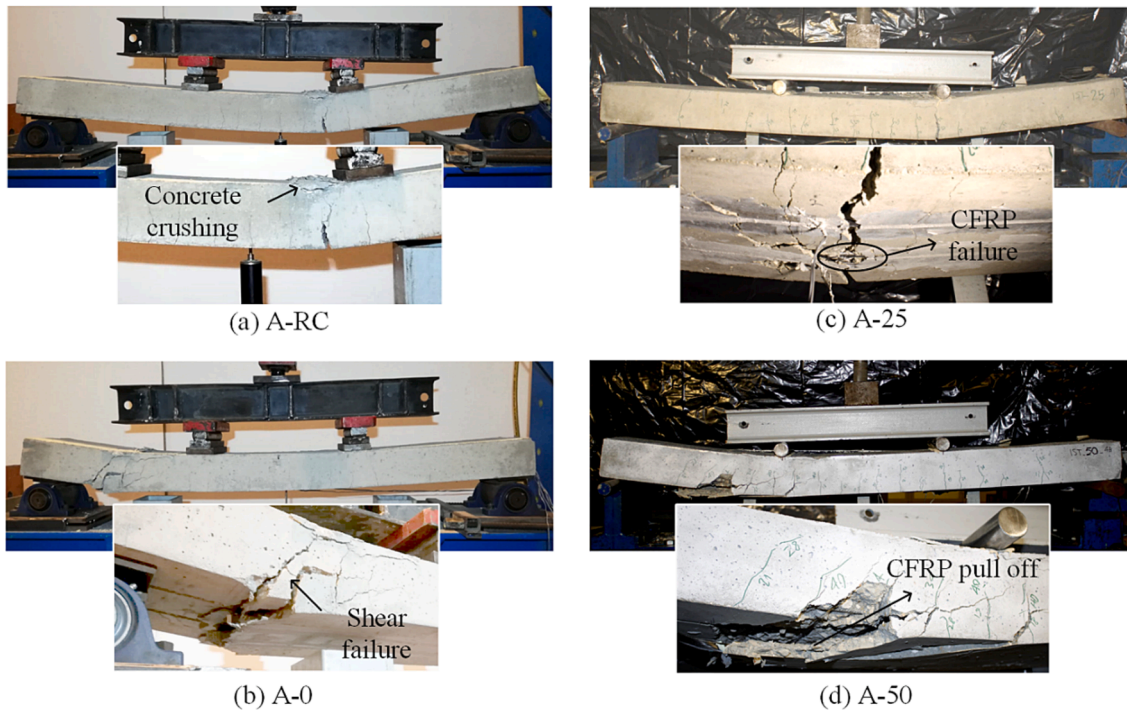


Fig. 5. Failure modes of specimens (a) A-RC, (b) A-0, (c) A-25 and (d) A-50.

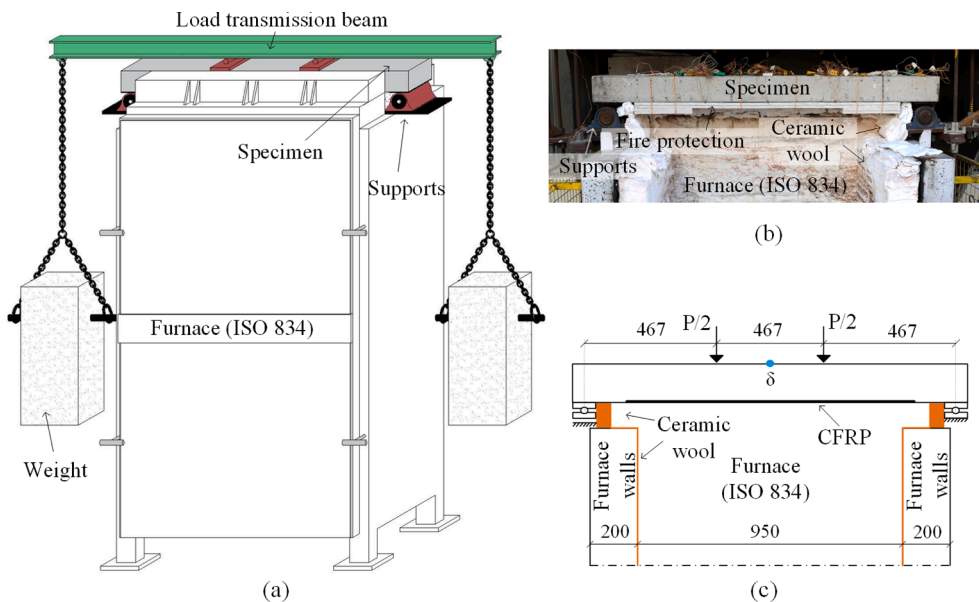


Fig. 6. Fire resistance test setup: (a) general view of the tests, (b) frontal view of a specimen with fire protection, prior to testing (furnace opened), and (c) longitudinal scheme of the tests. Dimensions in [mm].

3. Fire resistance tests

3.1. Test setup

For the fire resistance tests, the specimens were placed at the top of an intermediate scale furnace (external dimensions of 1.35 m length \times 1.20 m width \times 2.10 height), using the same four-point bending configuration adopted in the flexural tests at ambient temperature (Fig. 6c). The supports (10 cm wide \times 25 cm long) were placed on top of cylindrical hinges, positioned above the furnace's walls and suspended from a steel reaction frame through steel rods (Fig. 6a). The fire load (detailed in Section 3.2) was applied using a load transmission beam with two tubular profiles in contact with two steel plates (25 cm long \times 8 cm wide) placed on the top of the specimens' surface. In order to simulate a slab strip exposed to fire, the bottom face (i.e. the strengthened face) of the specimens was exposed to the ISO 834 fire curve [37], while their lateral faces were covered with ceramic wool. Although a few commercial fixation systems for fire protection boards are now available (e.g. involving the combination of cement based adhesives with steel expanding anchors, as described in [38]), for the sake of simplicity, in the present experimental campaign, the CS boards were bonded to the bottom face of the slab strips with fire resistance mastic, and mechanically fixed using steel wires spaced at \sim 200 mm, which were fixed on the specimens' top surface.

3.2. Structural fire load

The fire load (P_{fire}) was applied by suspending two sets of weights at the ends of the load transmission beam, which were kept constant during the fire resistance tests (Fig. 6a). The value of the fire load was calculated considering the recommendations from Eurocode 2, part 1-2 [39], assuming 70 % of the design load (P_d) at ambient temperature (Table 3). The design load at ambient temperature was calculated based on Eurocode 2, part 1-1 [40], and the design value of the CFRP strain at failure ($\epsilon_{fd} = 11.2\%$, for the strengthened specimens) was calculated according to ACI 440.2R-17 [34]. Table 3 presents the design loads at 20 °C (P_d), the experimental failure loads at ambient temperature (P_u), the fire loads (P_{fire}), and the ratios fire load/design load at 20 °C of the reference specimen (P_{fire}/P_d^{RC}) and fire load/experimental failure load at ambient temperature of the reference specimen (P_{fire}/P_u^{RC}) for the different specimens tested. Most guidelines recommend disregarding the contribution of FRP strengthening systems for safety verifications involving the fire load combination; thus, in these tests, the area of CFRP (two laminates for each strengthened specimen) was intentionally designed to provide a high flexural strength increase (about 80 % of failure load increase at ambient temperature, considering the design value of the material properties), in order to simulate a fire design scenario in which it is necessary to consider the contribution of the strengthening system to guarantee the necessary load carrying capacity to withstand the fire design load; as shown in Table 3, the design load capacity of the non-strengthened RC slab (P_d^{RC}) is not enough to safely withstand the fire load of the strengthened RC slabs (i.e. $P_d^{RC} < P_{fire}$ of

Table 3

Total load applied in the fire tests (P_{fire}), and relations with the corresponding design load (P_d) and failure load at ambient temperature (P_u), for all types of slabs tested.

Specimen	Design load at 20 °C, P_d (kN)	Failure load at ambient temperature, P_u (kN)	Fire load, P_{fire} (kN)	$\frac{P_{fire}}{P_d^{RC}}$	$\frac{P_{fire}}{P_u}$	$\frac{P_{fire}}{P_u^{RC}}$
RC	13.8	25.3	9.7	0.70	0.38	0.38
F-0		45.8			0.48	
F-25	31.1	43.9	21.8	1.58	0.50	0.86
F-50		44.2			0.49	

strengthened (F) slabs).

3.3. Instrumentation and test procedure

The specimens' temperatures were measured with thermocouples type K (external diameter of 1 mm), in target points of the various materials (concrete, steel, bonding adhesive/CFRP laminates), and in the air above the specimens' top surface (the nomenclature used is presented in Fig. 7). At midspan section, three thermocouples were placed in the concrete at different depths (T1, T2, and T4), one thermocouple was placed in the tensile steel rebar (T3), and three thermocouples were placed in the bonding adhesive at the bottom of the slit (T6), at mid-depth of the slit (T5), and at the top of the CFRP laminate (T7, Fig. 7a). Additionally, six thermocouples were placed at the anchorage zones, in the end, middle and beginning of the anchorage (three in each anchorage, T8 to T13, cf. Fig. 7b). The midspan displacement was measured with two electrical wire-displacement transducers (from TML, model CDP-500, with a range of 500 mm), positioned at the top surface (cold part) of the specimens, one in each extremity of the specimens' width. The vertical displacements of the supports were also measured with additional electrical displacement transducers.

The test procedure consisted of two phases: (i) application of structural fire load (P_{fire}), and (ii) application of thermal fire load (ISO 834 fire curve [37]). To ensure the stabilization of the midspan displacement, the fire exposure only begun after 10 min of the structural load application; after this, the specimens' bottom surface was exposed to the fire curve until the end of the fire tests. The tests were finished when the mechanical contribution of the CFRP strengthening system was lost.

4. Results and discussion

4.1. Temperature vs. time of fire exposure

Fig. 8 shows the evolution of temperatures in all tested specimens. The temperature inside the furnace ($T_{furnace}$) followed accurately the ISO 834 [37] time-temperature fire curve, with only slight relative differences, well within the allowed limits.

The temperatures at the bottom steel rebars (thermocouple T3, Fig. 8) presented the following behaviour in all tested specimens: (i) they increased linearly until approximately 100 °C, (ii) stabilizing at this temperature and presenting a small plateau, due to the water evaporation of the surrounding concrete, followed by (iii) a linear increase until the end of the test, reaching a maximum of 194 °C (specimen F-0-P) at the CFRP debonding instant (detected in Fig. 10, as discussed ahead) – according to Eurocode 2, part 1-2 [39], for such temperature the thermal induced degradation of the mechanical properties of steel is negligible.

In specimens with fire protection (Fig. 8d and e), the temperatures at the anchorage of the strengthening system (thermocouple T9) showed a much lower increase when comparing to the specimens without fire protection; this allowed the (protected) strengthening systems to behave like a cable – in these specimens, the temperature in the adhesive along the anchorage zones remained much lower than that at the midspan section (thermocouple T5) and, consequently, the anchorages remained effective for a longer period of time, maintaining the efficacy of the strengthening system even after the CFRP laminate detached at the midspan section – this “cable” mechanism, also reported in RC slabs with passive CFRP-strengthening systems [21–24], allowed to extend significantly the mechanical contribution of the CFRP laminates under fire exposure. This effect was observed not only for the specimen with passive strengthening, but also for the specimen with 50 % prestress level, in which the strengthening system remained effective for 123 min (cf. Table 4).

Fig. 8 and Table 4 also show that in all strengthened specimens, at the debonding instants, the average temperatures at the CFRP anchorage

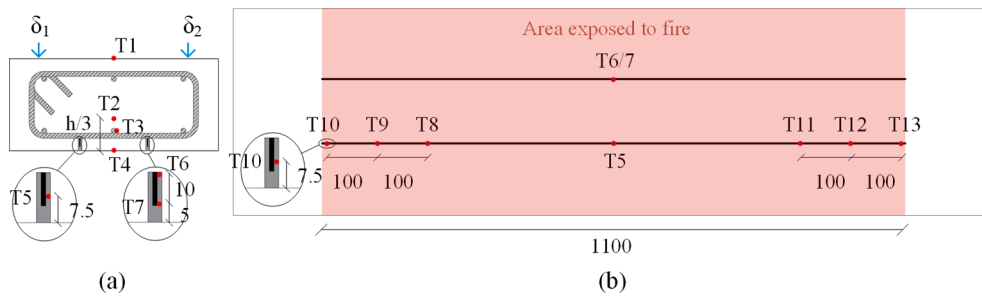


Fig. 7. Position of thermocouples (red) and displacement transducers (blue) at (a) midspan cross section and (b) anchorage zones of the CFRP laminates (not in scale). Dimensions in [mm]. (For interpretation of the references to colour in this figure legend, the reader is referred to the web version of this article.)

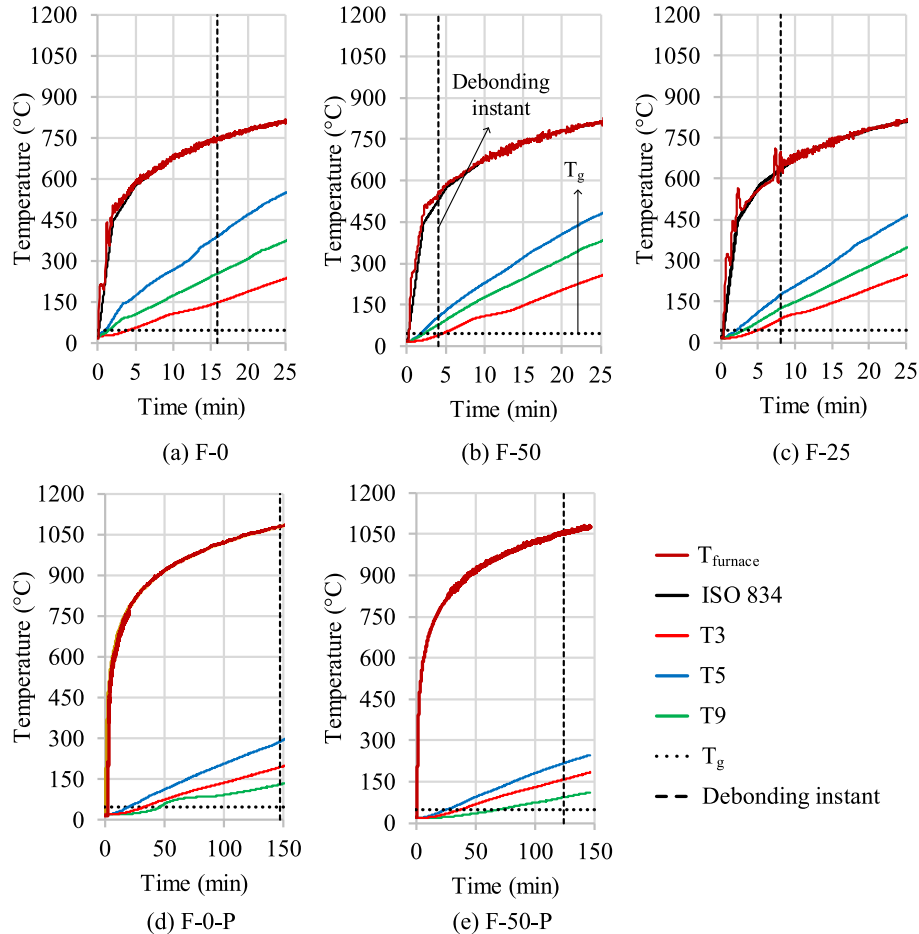


Fig. 8. Temperature vs. time of exposure for all tested specimens: (a) passive strengthening, (b) 50 % of prestress, (c) 25 % of prestress, (d) passive strengthening with fire protection, and (e) 50 % of prestress with fire protection.

zones were higher than the adhesive’s T_g , showing that it is possible to maintain the strengthening systems’ efficacy even after the bonding adhesive’s T_g is exceeded. However, when increasing the prestress level, these “critical” temperatures decrease (cf. Fig. 9), and this is associated to the reduction of the period of time for the CFRP laminate to detach completely. These aspects are discussed in further detail ahead.

4.2. Temperatures along the bonded interface when the strengthening system debonded

Fig. 9 compares the temperatures along the bonded interface of passive and prestressed-strengthened specimens, when the CFRP strengthening system lost its structural effectiveness (such instants were

detected on the midspan displacement vs. time curves, Fig. 10). Although most of the temperature distributions shown in Fig. 9 are as expected, in some specimens, there is a slight scatter in the results, which is attributed to: (i) the thermal gradient along the depth of the slits (e.g. at the debonding instant, the difference between the CFRP temperatures at the top (T6) and bottom (T7) of the slit for specimen F-0 was around 205 °C; (ii) the potential dragging of the thermocouples due to CFRP debonding (which was not fully instantaneous); (iii) the (local) effects of concrete cracking, which may contribute to the not fully symmetric distribution of temperatures.

As mentioned, the temperatures at the debonding instant decrease significantly when using NSM-CFRP prestressed systems (compared to non-prestressed), and the magnitude of such temperature decrease is

Table 4

Temperatures measured at the midspan section (steel rebars and adhesive) and at the anchorage zones (adhesive) when the CFRP laminate debonded, and corresponding instants.

Specimen	Temperatures at the midspan (°C)		Average temperatures at the anchorage zones (°C)	Debonding instant of the CFRP strengthening system (min)
	Tensile steel rebars (T3)	Adhesive (T5)		
F-0	145	384	134	16
F-0-P	194	241	154	147
F-25	86	174	117	8
F-50	40	105	73	4
F-50-P	157	215	88	123

more pronounced when the prestress level increases – this influence of the prestress level is logical, being attributed to (i) the higher stress level at the CFRP laminate and, consequently, at the concrete-adhesive-CFRP interface, and (ii) the bond strength reduction with temperature of such interface. Regarding the influence of fire protection, when applying CS boards with 48 mm of thickness in the anchorage zones and 24 mm of thickness in the central part of the span, the CFRP strengthening system remained effective for considerably longer periods of fire exposure, which increased by 131 min and 119 min when compared to unprotected specimens F-0-P and F-50-P, respectively, even though the temperature at the midspan section at the debonding instant was much higher than the adhesive's T_g (241 °C and 215 °C vs. 46 °C, for specimens F-0-P and F-50-P, respectively). When using this type of fire protection (thicker layers in the anchorage zones and thinner layers in the centre of

the span), it is possible to take advantage of the above-mentioned cable mechanism; as shown earlier [22,24], when applying this type of fire protection, the fire resistance improves significantly even if the adhesive's T_g is highly exceeded in the centre of the span, since in the anchorage zones the temperature increase is much less pronounced and therefore the CFRP laminates remain well anchored.

4.3. Midspan displacement with time of fire exposure

Fig. 10 shows for all specimens the evolution of the midspan displacement as a function of the time of fire exposure. It is possible to see the debonding instants of the NSM-CFRP systems, corresponding to sudden increases in the midspan deflection – in some specimens it is possible to see two midspan displacement increases, showing that the two CFRP laminates of each specimen debonded at different instants; nevertheless, those instants were always less than 9 min apart and more evident in specimens with fire protection, possibly due to the delayed thermal degradation of the CFRP-adhesive-concrete interface.

As mentioned, with the increase in the prestress level, the time during which the CFRP system remained effective decreased, namely from 16 min (F-0) to 4 min (F-50) in specimens without fire protection. Once more, with fire protection, not only the time to debonding increased significantly, but also the midspan displacement rate was much lower compared to that of specimens without fire protection; this was naturally due to the thermal insulation conferred by the CS boards, which delayed the thermal induced degradation of the materials and interfaces, regardless of the prestress level.

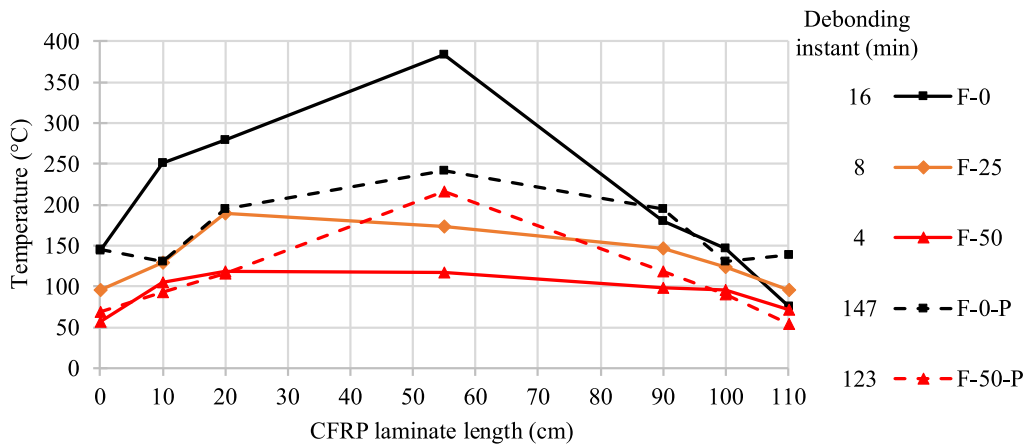


Fig. 9. Temperatures in the adhesive when the CFRP laminates debonded.

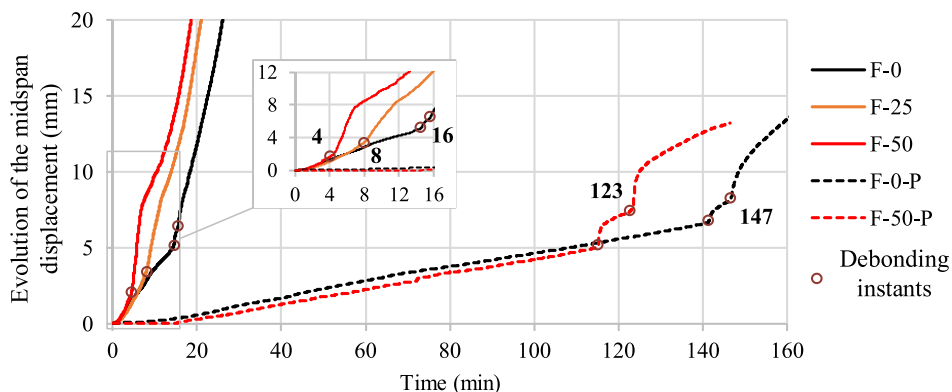


Fig. 10. Evolution of the midspan displacement vs. time of fire exposure. Debonding instants marked in brown.

4.4. Failure modes and structural effectiveness of strengthening system

Fig. 11 shows the post-fire assessment of representative unprotected and protected specimens. In unprotected specimens (F-0, F-25, and F-50), significant thermal degradation of the bonding adhesive was observed at the end of the tests, whereas in protected specimens (F-0-P and F-50-P), the degradation of the bonding adhesive was less severe, due to the insulation provided by the fire protection system, which remained intact throughout the fire tests. In fact, as also shown in [24], the integrity of the fixation is crucial to ensure the effectiveness of the fire protection; thus, further investigations are needed to study the effectiveness of available commercial fixation methods for CS boards. Nevertheless, in all specimens, the CFRP system failed due to loss of adhesion between the CFRP laminates and concrete (CFRP debonding), indicating that the efficacy of the strengthening system under fire exposure was governed by the temperature attained at the bonding adhesive.

Fig. 12 shows the initial tensile stresses in the CFRP laminates installed in all specimens (i.e. due to the prestress level and the fire load applied, P_{fire}), marked as horizontal lines, together with the degradation of their tensile strength, estimated at each instant (x_i), based (i) on the temperatures measured in the material at those instants (T_{x_i} in °C) and (ii) the remaining tensile strength with temperature ($f_{fu}(T_{x_i})$), as proposed by Yu and Kodur [41] (for temperatures up to 900 °C), according to the following expression.

$$f_{fu}(T_{x_i}) = 0.56 - 0.44 \tanh(0.0052(T_{x_i} - 305)) \quad (1)$$

It is shown that for all specimens the temperature-dependent tensile strength of the CFRP laminates always remained higher than the initial stress level in the CFRP laminates; this helps explaining why CFRP tensile failure did not occur, even in specimens with the highest prestress level. Nevertheless, it is worth mentioning that the stresses in the CFRP laminates at the debonding instant were caused not only by the prestress level and the fire (mechanical) load, but also by the thermal gradient installed in the cross-section (due to one-side heating), and the consequent midspan deflection increase with the temperature rise.

Fig. 13 shows the comparison of the fire performance of all specimens tested, with passive and prestressed CFRP laminates, in terms of (i) time of fire exposure until the CFRP strengthening system lost its efficacy (Fig. 13a), corresponding to the debonding of both CFRP laminates (cf. Fig. 9), and (ii) minimum average temperature in the adhesive along the anchorage zones at the debonding instant (Fig. 13b). As mentioned, the period of time during which the CFRP strengthening system remained effective decreased with the prestress level increase: when no fire protection was used, the reductions were 8 min for 25 % of prestress (from 16 min to 8 min) and 12 min for 50 % of prestress (from 16 min to

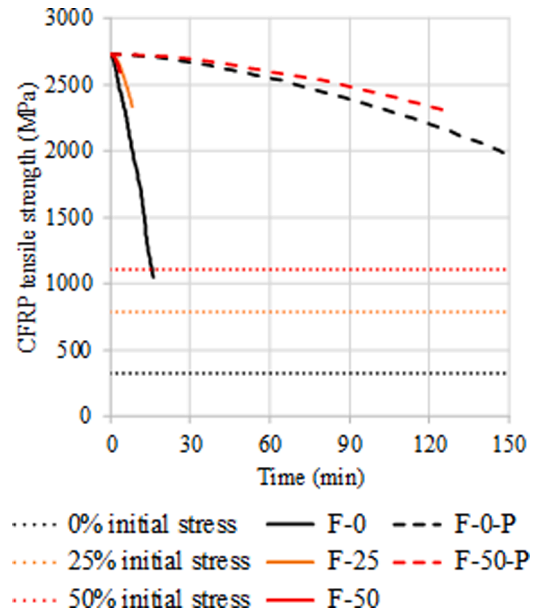


Fig. 12. Temperature-dependent reduction of tensile strength of CFRP laminates with the time of fire exposure (predicted), and initial stresses in the CFRP for all specimens tested.

4 min), confirming the increased susceptibility of prestressed CFRP strengthening systems. With the fire protection system adopted in the experiments, for 50 % of prestress, the reduction was 24 min (from 147 min to 123 min). Nevertheless, the time of fire exposure of the fire protected strengthening systems are higher than 120 min (namely 123 min and 147 min, respectively for specimen F-50-P and F-0-P), fulfilling the requirements set for most types of buildings [42].

Regarding the critical temperatures of the various specimens, defined as the minimum average temperature at the adhesive along the anchorage zone when the strengthening system lost its effectiveness, Fig. 13b shows the following figures: in passive strengthened specimens (F-0 and F-0-P), the CFRP debonded for average temperatures in the anchorage zones from $2.9T_g$ to $3.4T_g$, considerably higher than the adhesive's T_g – these results are within the range previously reported in [22] for passive NSM technique, in which these temperatures varied between $2.5T_g$ and $5.1T_g$; whereas for prestressed strengthened specimens (F-25, F-50 and F-50-P), this critical temperature range was lower, with a decreasing trend with the prestress level increase, ranging from $2.5T_g$ to $3.0T_g$ for 25 % of prestress, and from $1.6T_g$ to $2.2T_g$ for 50 % of

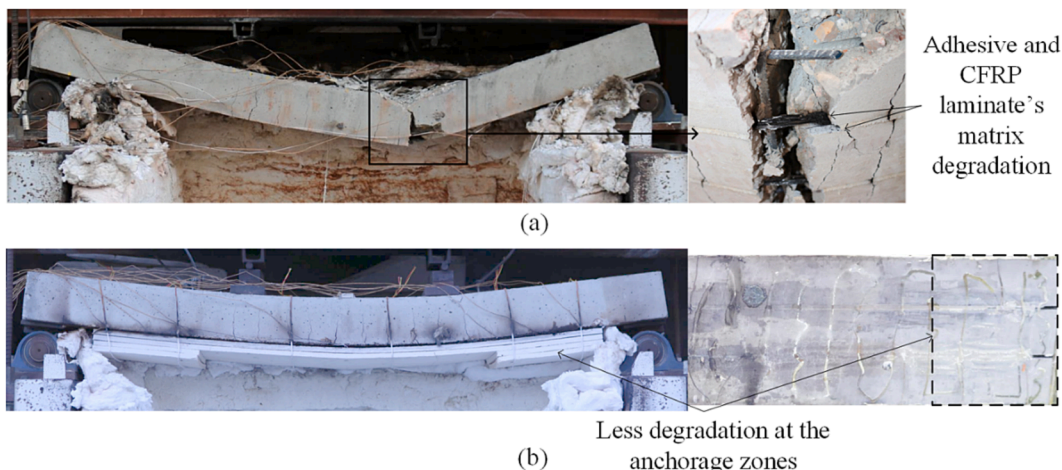


Fig. 11. Post-fire assessment of (a) unprotected specimens (F-0, F-25, F-50), and (b) protected specimens (F-0-P, F-50-P).

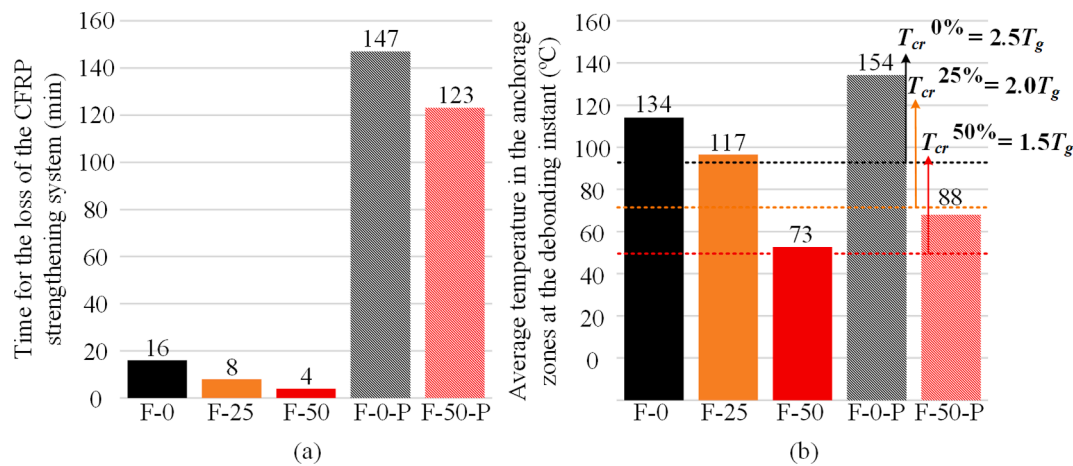


Fig. 13. (a) Fire resistance of the strengthening systems, and (b) minimum average temperature in the anchorage zones when the CFRP debonded – “critical” temperatures defined by the dashed lines for each prestress level (black, orange and red for 0 %, 25 % and 50 %, respectively). (For interpretation of the references to colour in this figure legend, the reader is referred to the web version of this article.)

prestress.

Considering the results obtained and for the materials used in the present experimental campaign, and based on an engineering judgement, the following “critical” temperatures are proposed for prestressed-NSM-CFRP strengthening systems: $2.5T_g$ for passive CFRP laminates, and $2.0T_g$ and $1.5T_g$ for CFRP laminates with prestress levels of respectively 25 % and 50 % of the CFRP strength. It important to mention that these “critical” temperatures are a lower bound of the minimum average temperatures measured at the anchorage zones and, despite being conservative estimates, they lack a reliability analysis.

5. Conclusions

This paper presented the results of an experimental study about the fire resistance behaviour of RC slab strips strengthened with prestressed-NSM-CFRP laminates. The following main conclusions are drawn:

1. The tests highlighted the increased susceptibility to fire of specimens strengthened with prestressed systems: without fire protection, comparing to the passive strengthened specimen, the period of time during which the CFRP system remained effective decreased from 16 min to 8 min and 4 min for specimens with 25 % and 50 % of prestress level, respectively.
2. The presence of fire protection highly increased the period of time during which the CFRP system remained effective, which was 147 min and 123 min for 0 % and 50 % of prestress level, respectively.
3. The minimum average temperatures in the anchorage zones at the debonding instant consistently decreased with the prestress level, ranging between $1.6T_g$ and $2.2T_g$ for 50 % of prestress, between $2.5T_g$ and $3.0T_g$ for 25 % of prestress, and between $2.9T_g$ and $3.4T_g$ with passive strengthening. Considering these temperatures and based on engineering judgement, the following critical temperatures for the CFRP anchorage zones are proposed: $2.5T_g$, $2.0T_g$ and $1.5T_g$ for passive CFRP laminates, and for 25 % and 50 % of prestress, respectively.

Declaration of Competing Interest

The authors declare that they have no known competing financial interests or personal relationships that could have appeared to influence the work reported in this paper.

Data availability

Data will be made available on request.

Acknowledgments

The authors wish to acknowledge FCT (project FireComposite PTDC/ECM-EST/1882/2014 and CERIS project UIDB UIDB/04625/2020); Secil and Unibetão for supplying the concrete; and S&P Clever Reinforcement for supplying the CFRP laminates and the epoxy adhesive. The first author also wishes to thank the financial support of FCT through the scholarship SFRH/BD/145256/2019.

References

- [1] Correia JR. Fibre-reinforced polymer (FRP) composites. *Mater Constr Civ* 2015; 501–56. <https://doi.org/10.1007/978-3-319-08236-3>.
- [2] Motavalli M, Czaderski C. FRP composites for retrofitting of existing civil structures in Europe: state-of-the-art review. *Am Compos Manuf Assoc* 2007:1–10.
- [3] Barros JAO, Dias SJE, Lima JLT. Efficacy of CFRP-based techniques for the flexural and shear strengthening of concrete beams. *Cem Concr Compos* 2007;29:203–17. <https://doi.org/10.1016/j.cemconcomp.2006.09.001>.
- [4] Ceroni F. Experimental performances of RC beams strengthened with FRP materials. *Constr Build Mater* 2010;24:1547–59. <https://doi.org/10.1016/j.conbuildmat.2010.03.008>.
- [5] Bilotta A, Ceroni F, Di Ludovico M, Nigro E, Pecce M, Manfredi G. Bond efficiency of EBR and NSM FRP systems for strengthening concrete members. *J Compos Constr* 2011;15:757–72. [https://doi.org/10.1061/\(asce\)cc.1943-5614.0000204](https://doi.org/10.1061/(asce)cc.1943-5614.0000204).
- [6] Sena-Cruz JM, Barros JAO, Coelho MRF, Silva LFFT. Efficiency of different techniques in flexural strengthening of RC beams under monotonic and fatigue loading. *Constr Build Mater* 2011;29:175–82. <https://doi.org/10.1016/j.conbuildmat.2011.10.044>.
- [7] Firmo JP. Fire behaviour of reinforced concrete structures strengthened with CFRP strips. Universidade de Lisboa; 2015. PhD Thesis in Civil Engineering.
- [8] Zhang Y, Elsayed M, Zhang LV, Nehdi ML. Flexural behavior of reinforced concrete T-section beams strengthened by NSM FRP bars. *Eng Struct* 2021;233:111922. <https://doi.org/10.1016/j.engstruct.2021.111922>.
- [9] Badawi M, Soudki K. Flexural strengthening of RC beams with prestressed NSM CFRP rods – experimental and analytical investigation. *Constr Build Mater* 2009; 23:3292–300. <https://doi.org/10.1016/j.conbuildmat.2009.03.005>.
- [10] Hajihashemi A, Mostofinejad D, Azhari M. Investigation of RC beams strengthened with prestressed NSM CFRP laminates. *J Compos Constr* 2011;15:887–95. [https://doi.org/10.1061/\(ASCE\)CC.1943-5614.0000225](https://doi.org/10.1061/(ASCE)CC.1943-5614.0000225).
- [11] Rezazadeh M, Costa I, Barros J. Assessment of the effectiveness of prestressed NSM CFRP laminates for the flexural strengthening of RC slabs. *Compos Struct* 2014; 111:249–58. <https://doi.org/10.1016/j.compstruct.2013.12.018>.
- [12] El-Hacha R, Soudki K. Prestressed near-surface mounted fibre reinforced polymer reinforcement for concrete structures - a review. *Can J Civ Eng* 2013;2013: 1127–39. <https://doi.org/10.1139/cjce-2013-0063>.
- [13] Costa I, Rezazadeh M, Barros J. Evaluation of the performance of full-scale RC beams prestressed with NSM-CFRP laminates. In: 7th Int. Conf. FRP Compos. Civ. Eng. CICE 2014, Vancouver, Canada; 2014. p. 1–6.

- [14] Rezazadeh M, Costa I, Barros J. Influence of prestress level on NSM CFRP laminates for the flexural strengthening of RC beams. *Compos Struct* 2014;116:489–500. <https://doi.org/10.1016/j.compstruct.2014.05.043>.
- [15] Hosseini MRM, Dias SJE, Barros JAO. Effectiveness of prestressed NSM CFRP laminates for the flexural strengthening of RC slabs. *Compos Struct* 2014;111:249–58. <https://doi.org/10.1016/j.compstruct.2013.12.018>.
- [16] Elharouney O, Elkateb M, Khalil A. Behaviour of prestressed hollow core slabs strengthened with NSM CFRP strips around openings: a finite element investigation. *Eng Struct* 2021;238:112262. <https://doi.org/10.1016/j.engstruct.2021.112262>.
- [17] Azevedo AS, Firmo JP, Correia JR, Tiago C. Influence of elevated temperatures on the bond behaviour between concrete and NSM-CFRP strips. *Cem Concr Compos* 2020;111:103603. <https://doi.org/10.1016/j.cemconcomp.2020.103603>.
- [18] Mouritz AP, Gibson AG. *Fire properties of polymer composite materials*, Vol. 143. Springer; 2006.
- [19] Firmo JP, Correia JR, Bisby LA. Fire behaviour of FRP-strengthened reinforced concrete structural elements: a state-of-the-art review. *Compos Part B: Eng* 2015;80:198–216. <https://doi.org/10.1016/j.compositesb.2015.05.045>.
- [20] Firmo JP, Roquette MG, Correia JR, Azevedo AS. Influence of elevated temperatures on epoxy adhesive used in CFRP strengthening systems for civil engineering applications. *Int J Adhes Adhes* 2019;1–11. <https://doi.org/10.1016/j.ijadhadh.2019.01.027>.
- [21] Jiangtao Y, Yichao W, Kexu H, Kequan Y, Jianzhuang X. The performance of near-surface mounted CFRP strengthened RC beam in fire. *Fire Saf J* 2017;90:86–94. <https://doi.org/10.1016/j.firesaf.2017.04.031>.
- [22] Firmo JP, Correia JR. Fire behaviour of thermally insulated RC beams strengthened with NSM-CFRP strips: experimental study. *Composites: Part B* 2015;76:112–21. <https://doi.org/10.1016/j.compositesb.2015.02.018>.
- [23] Zhu H, Wu G, Zhang L, Zhang J, Hui D. Experimental study on the fire resistance of RC beams strengthened with near-surface-mounted high - Tg BFRP bars. *Composites: Part B* 2014;60:680–7. <https://doi.org/10.1016/j.compositesb.2014.01.011>.
- [24] Azevedo AS, Firmo JP, Correia JR, Chastre C, Biscaia H, Franco N. Fire behaviour of CFRP-strengthened RC slabs using different techniques – EBR, NSM and CREAtE. *Compos Part B: Eng* 2021:109471. <https://doi.org/10.1016/j.compositesb.2021.109471>.
- [25] Al-Abdwais AH, Al-Mahaidi RS. Evaluation of high temperature endurance of RC beams retrofitted with NSM technique using CFRP composites and modified cement-based adhesive. *Eng Struct* 2022;264:114445. <https://doi.org/10.1016/j.engstruct.2022.114445>.
- [26] López C, Firmo JP, Correia JR, Tiago C. Fire protection systems for reinforced concrete slabs strengthened with CFRP laminates. *Constr Build Mater* 2013;47:324–33. <https://doi.org/10.1016/j.conbuildmat.2013.05.019>.
- [27] EN 197-1. Cement - Part 1: composition, specification and conformity criteria for common cements. European Committee for Standardization, Brussels, Belgium; 2000.
- [28] EN 12390-3. Testing hardened concrete - Part 3: compressive strength of test specimens. Brussels, Belgium: European Committee for Standardization; 2009.
- [29] EN 12390-6. Testing hardened concrete - Part 6: tensile splitting strength of test specimens. Brussels, Belgium: European Committee for Standardization; 2009.
- [30] EN 10002-1. Metallic materials - tensile testing - Part 1: method of test at ambient temperature. Brussels, Belgium: European Committee for Standardization; 2001.
- [31] MohammadiFirouz R, Pereira ENB, Barros JAO. Bond performance of NSM – CFRP laminates using different surface treatments and cementitious adhesives; 2019. p. 3–6.
- [32] ISO 527-5. Plastics - determination of tensile properties - Part 5: test conditions for unidirectional fibre-reinforced plastic composites. Genève, Switzerland; 2009.
- [33] ISO 527-2. Plastics - determination of tensile properties - Part 2: test conditions for moulding and extrusion plastics. Geneva, Switzerland; 2012.
- [34] *ACI Committee 440. Guide for the design and construction of externally bonded FRP systems for strengthening concrete structures*. Farmington Hills, MI, USA: American Concrete Institute; 2017.
- [35] *ACI Committee 440. Prestressing concrete structures with FRP tendons*. Farmington Hills, MI, USA: American Concrete Institute; 2004.
- [36] Hosseini MRM, Dias SJE, Barros JAO. Flexural strengthening of reinforced low strength concrete slabs using prestressed NSM CFRP laminates. *Composites: Part B* 2016;90:14–29. <https://doi.org/10.1016/j.compositesb.2015.11.028>.
- [37] ISO 834-1. Fire resistance tests-elements of building construction-Part 1: general requirements. Geneva, Switzerland: International Organization for Standardization; 1999.
- [38] Reinforcement Systems on Concrete Decks and Beams PROMATECT® - L500 Protection to Epoxy Bonded, Technical Data Sheet – 117; 2009.
- [39] EN 1992-1-2. Eurocode 2: design of concrete structures - Part 1-2: general rules - structural fire design. European Committee for Standardization, Brussels, Belgium; 2010.
- [40] EN 1991-1-1. Eurocode 2: design of concrete structures - Part 1-1: general rules and rules for buildings. Brussels, Belgium: European Committee for Standardization; 2010.
- [41] Yu B, Kodur VKR. Effect of high temperature on bond strength of near-surface mounted FRP reinforcement. *Compos Struct* 2014;110:88–97. <https://doi.org/10.1016/j.compstruct.2013.11.021>.
- [42] Lamalva K, Hopkin D. *International handbook of structural fire engineering*. Springer; 2021.